

Interface formation and growth of InSb on Si(100)

G. E. Franklin, D. H. Rich,* Hawoong Hong, T. Miller, and T.-C. Chiang

*Department of Physics, University of Illinois at Urbana-Champaign, 1110 West Green Street, Urbana, Illinois 61801
and Materials Research Laboratory, University of Illinois at Urbana-Champaign, 104 South Goodwin Avenue, Urbana, Illinois 61801*

(Received 25 July 1991)

High-energy electron diffraction, Auger spectroscopy, photoemission, and x-ray diffraction were used to study the interface and subsequent growth of InSb on vicinal (4° off) and on-axis Si(100). During the initial stages of molecular-beam epitaxy at 410°C , we examined the In, Sb, and Si core levels as a function of In and Sb coverage and deposition order. Based on these results, a model for interface formation is developed. Thicker coverage results of coevaporated InSb are discussed in light of the interfacial analyses.

I. INTRODUCTION

Interface formation and growth of compound semiconductors on silicon has been the subject of much interest. From a technological viewpoint the integration of these two categories of semiconductors combines the optical and electronic performance of III-V semiconductors with complex silicon integrated circuitry. From a fundamental viewpoint the interesting questions lie in the geometric and electronic structure of the chemical bonds at the interface. By investigating the initial interfacial interactions, questions concerning deviations from ideal epitaxial growth because of surface phenomena such as defect and step morphology, surface reconstructions, and adsorbate-to-substrate bonding can be addressed. Device performance, in turn, depends on the ability to grow high-quality epitaxial films free of defects and dislocations. Hence the construction of many optimal devices is directly linked to the details at the interface.

Previous experimental and theoretical studies of the surface kinetics of III-V materials on Si(100) mostly concentrated on the GaAs/Si(100) system.¹⁻⁵ Despite the 4% lattice mismatch and differing thermal-expansion coefficients, high-quality GaAs films were grown with most of the dislocations occurring near the interface.⁶ In addition, later publications showed that the antiphase disorder problem, because of the two domains on Si(100), could be eliminated by growing on vicinal Si(100) with between a 2° - 4° tilt in the [011] direction.⁷ Microscopic analysis of these GaAs films on Si(100) has utilized core-level spectroscopy,¹ cross-sectional transmission electron microscopy,⁸ and high-energy electron diffraction (HEED).⁹

For our present study we use molecular-beam epitaxy (MBE), which is an ideal growth technique for submonolayer and thick-layer systems because of its highly controllable nature (i.e., for III-V materials the deposition order, flux ratio, and growth rate can be very important for growing quality films). Synchrotron core-level photoemission, HEED, Auger spectroscopy, and x-ray diffraction provide the principal results for the evolution of InSb on Si(100) and vicinal (4° -off) substrates. One can imagine that a major difficulty in growing InSb on Si would be the rather large lattice mismatch between these

two materials—about 19%. In an earlier report the growth kinetics of InSb thin films on on-axis Si(100) substrates were investigated.¹⁰ Based on HEED and relative desorption rates of In and Sb, InSb heteroepitaxial films were thought to have been grown in the temperature range between 427°C and 607°C , even past the 535°C melting temperature of InSb. There was no discussion of the bonding at the interface, the actual InSb film thicknesses grown, or the quality and composition of the InSb films. We will try to discuss these as well as other criteria involved in the initial growth of InSb films. Thicker-coverage results will be discussed in light of the interfacial results.

II. EXPERIMENTAL DETAILS

The photoemission experiments were carried out using synchrotron radiation from the University of Illinois beam line on the 1-GeV storage ring Aladdin at the Synchrotron Radiation Center of the University of Wisconsin. Light from the ring was dispersed by an extended-range grasshopper monochromator. Our core-level spectroscopy experiments utilized a Leybold EA-10/100 hemispherical analyzer. The sample Fermi level was measured from a polycrystalline Au foil in electrical contact with the Si samples. These spectra indicated an overall system resolution of 150–250 meV, depending on the photon energy used. The relative binding energies of each spectrum are referenced to the Fermi level. The Auger experiments were performed *in situ* with a Perkin-Elmer Auger system, and the x-ray-diffraction data were taken with a fixed-anode Rigaku/D-MAX system and Cu $K\alpha$ radiation.

All of the samples used in this study were from standard commercial *n*-type Si(100) ($\leq 0.5^\circ$ miscut) or vicinal Si(100) (4° off, roughly 2° toward $[0\bar{1}1]$ and 3° toward $[011]$ from the $[100]$ normal direction), having a resistivity of about $10\ \Omega\text{ cm}$. Cut samples were then placed in our vacuum chamber, with a base pressure better than 10^{-10} torr and cleaned by heating with direct current to about 1060°C for 10 s. The surface was then checked *in situ* using HEED, which revealed a sharp two-domain (2×1) for the on-axis samples and a sharp one-domain (2×1) for the vicinal surfaces. MBE was then accom-

plished through evaporation from electron-beam-heated crucibles containing 99.999% pure In and Sb. The rate of deposition for each material was monitored using a quartz-crystal thickness monitor. One monolayer (ML) of In or Sb is defined as 6.8×10^{14} atoms/cm², which is the site-number density for the unreconstructed Si(100) surface.

III. RESULTS AND DISCUSSION

A. Low coverages

The main questions we focused on during the first couple of monolayers of InSb growth were whether In or Sb or both formed the first layer on Si and how the next layer proceeded to interact with the first. Also, since it was found that GaAs forms three-dimensional islands that nucleate from step edges on Si(100),^{4,8,11} we decided to check for any differences that growing on vicinal Si(100) might make as compared with the on-axis substrate.

For growing InSb on InSb(100), the substrate temperature should be held between 260°C and 450°C.^{12,13} This is also roughly the temperature range for growing InSb films on other substrates such as CdTe (Ref. 14) and GaAs.¹⁵ For the initial submonolayer growth of InSb on Si(100), HEED and Auger spectroscopy showed no noticeable InSb growth differences between 350°C and 500°C, and so we chose to maintain our sample temperature at about 410°C. The deposition rate of either In or Sb was kept at around 1 ML per minute during evaporation.

1. Results

Both In/Si(100) (Refs. 16 and 17) and Sb/Si(100) (Refs. 18 and 19) have been studied before in the above temperature spread. Sb behaves much differently than In on Si(100) and does not form a stable reconstruction. Upon Sb adsorption, HEED showed the $\frac{1}{2}$ -order spots of the clean Si(100)-(2×1), diminishing until at $\frac{1}{2}$ -ML coverage only the (1×1) bulk spots on top of a high background were apparent. The background seemed to increase until the 1-ML saturation coverage, where the sticking coefficient of Sb drops to zero.¹⁹ The result was a disordered Sb-terminated surface.¹⁸ For In deposition, a (3×4) pattern is observed at $\frac{1}{2}$ -ML coverage, and any additional In deposition on the surface forms three-dimensional metallic balls.¹⁶ After Sb exposures on this 1-ML In-covered surface, a steady degradation of the (3×4) occurs with an increasing background. At $\frac{1}{2}$ -ML Sb exposure only (1×1) spots appear on top of a high background, very similar to the diffraction pattern for $\frac{1}{2}$ ML Sb on clean Si. Further Sb exposures did not have any more noticeable effect, except maybe a slight increase in the background.

For our photoemission experiment, a surface-sensitive photon energy was used for each of the core levels. The surface shifts and intensities of the various components were determined by following a fitting procedure described previously.^{20,21} We begin with Fig. 1, which shows the evolution of the In 4d core level. The experimental results (open circles), overall fit (solid curve), and

two background-subtracted surface components S1 and S2 (medium- and short-dashed curves) are shown. Each spectrum for a given In and Sb exposure is shown relative to the initial exposure at the bottom of the graph and referenced to the Fermi level. Deposition order is shown in the two columns from left to right. We initially deposited 1 ML In on the clean Si(100)-(2×1) surface, and then varying amounts of Sb were deposited next. It should be mentioned that the relative intensities between different exposures are not meaningful; they will be displayed in a separate figure.

Figure 2 shows the similarly analyzed Sb 4d core level for the same deposition order. Only one surface component was found.

The intensity ratios, for both the In and Sb cores with respect to the Si core, are shown in Fig. 3. Experimentally, intensity ratios can be measured more accurately than absolute intensities, because precise sample repositioning in front of the analyzer and synchrotron beam after each growth is not required. The In 4d higher binding-energy surface component S1 (circle), the lower-binding-energy surface component S2 (triangle), and the Sb 4d surface component S1 (square) are plotted versus various Sb exposures. On this scale the values of $I_{\text{Sb}}/I_{\text{Si}}$ are reduced to make it comparable to the values of $I_{\text{In}}/I_{\text{Si}}$ since the cross section for Sb is so much larger than In for these photon energies. So, after $\frac{1}{2}$ ML of Sb exposure, the In

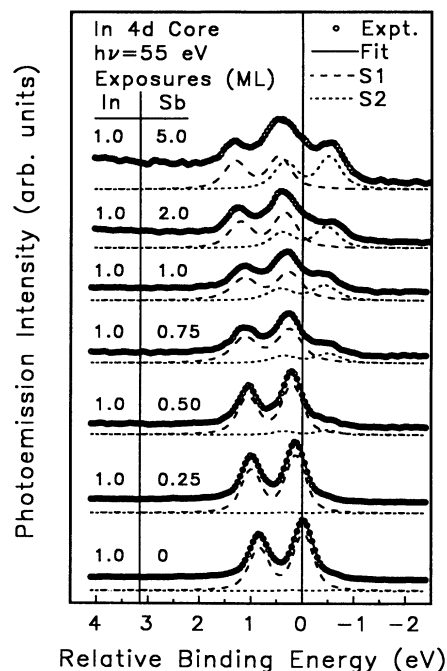


FIG. 1. In 4d core-level spectra (open circles) taken with a photon energy of 55 eV. Successive Sb exposures deposited on a 1-ML-In-covered Si(100) surface are indicated for each spectrum. The solid curves are a result of a fit to the data. The decompositions of the spectra into the two surface contributions S1 and S2 are shown by the medium- and short-dashed curves, respectively. The relative binding energies are referenced to the Fermi level, which is located at -17.4 ± 0.1 eV.

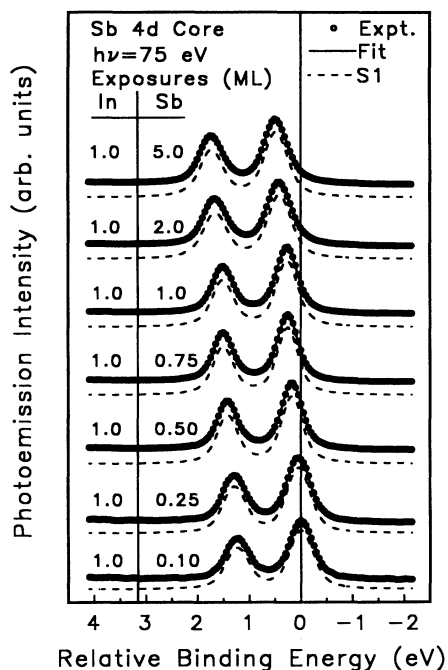


FIG. 2. Sb 4d core-level spectra (open circles) taken with a photon energy of 75 eV. Successive Sb exposures deposited on a 1-ML-In-covered Si(100) surface are indicated for each spectrum. The solid curves are a result of a fit to the data. The spectra can be fit by just one surface contribution S1, as shown by the medium-dashed curves.

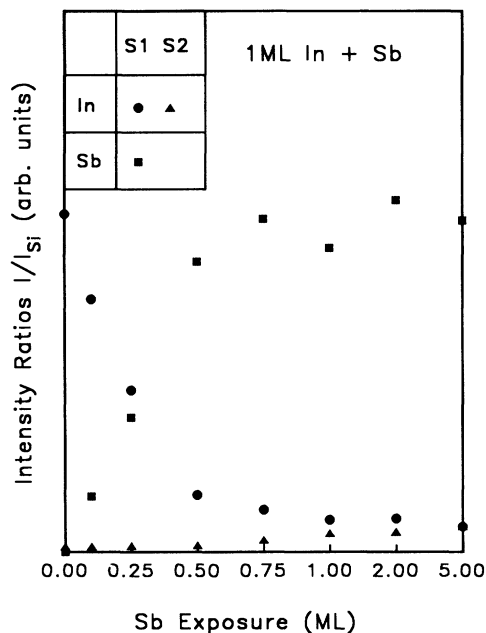


FIG. 3. In and Sb intensity ratios for each surface component, with respect to the Si bulk, are shown for various Sb exposures on a 1-ML-In covered Si(100) surface. Circles and triangles indicate the results for the two In surface components. Squares show similar results for the Sb surface site.

S1 component is reduced to roughly 15–20% ($\approx \frac{1}{10}$ ML) of its value before any Sb had been deposited. In Figs. 1–3 the data shown were taken on on-axis Si(100) samples. Several spectra of the identical exposures but deposited on vicinal Si(100) were recorded. Since there were no obvious differences in terms of either line shape or intensity, these spectra are not shown.

The Si 2p core was analyzed in Fig. 4, which shows a few typical spectra relative to the clean Si(100)-(2 \times 1) surface. For the clean surface, the decomposition of these spectra into the bulk (B) and surface (S) contributions is shown by the medium- and short-dashed curves, respectively. For the covered surfaces (top three spectra), the surface-shifted component is suppressed. This effect has been seen before for Sb/Si(100) (Ref. 18) and for the low-temperature growth phase of In/Si(100).²²

Figures 5–7 are similar to Figs. 1–3 except for two main differences. The data shown on these were taken on vicinal Si(100), and the deposition order begins with 1 ML Sb and continues with increasing In exposures. Again, several spectra of the identical exposure ordering were taken on on-axis Si(100) substrates, but since there were no obvious differences in line shape or intensity, these spectra are not shown.

Figures 8, 9, and 10 show the evolution as a function of In coverage of the In core level, Sb core level, and $I_{\text{In}}/I_{\text{Si}}$ and $I_{\text{Sb}}/I_{\text{Si}}$ intensity ratios, respectively. This was done for an initial 40-ML Sb exposure followed by a few In

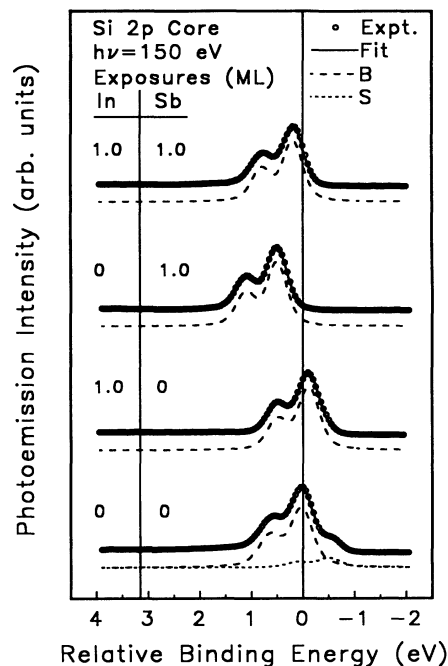


FIG. 4. Si 2p core-level spectra (open circles) taken with a photon energy of 150 eV. Independent Sb and In exposures are listed with the decomposition of the Si spectrum into bulk (medium-dashed curve) and surface component (short-dashed curve). The relative binding energies are referenced to the Fermi level, which is located at -98.7 ± 0.1 eV.

coverages. Again, the core levels were deconvoluted and the results were somewhat similar to those in the previous sets.

2. Core-level analysis

For the In core level in Fig. 1, we note two trends. First, there is a band-bending effect causing the *S1* core-level binding energies to increase toward higher binding energy with Sb exposures. These spectra are presented with the Fermi level as the reference. The observed band bending, with respect to the clean surface, is 0.2 eV at 1 ML In + 1 ML Sb and moves to 0.4 eV at higher Sb coverages (see the top spectrum in Fig. 1). For comparison, a previous study shows a 0.55-eV band bending at 1-ML Sb coverage on Si(100) and a saturation band bending of 0.63 eV at higher Sb coverages.²³ The present values are less since there is some In on the surface, which tends to bend the bands in the opposite direction (In is an acceptor and Sb is a donor in silicon). Second, a second surface site *S2*, at lower binding energy, seems to emerge with increasing Sb exposure (see Fig. 3) and remains fixed to the Fermi level. The *S2* site is actually visible even in the initial 1-ML In coverage. Indium is known to clump together on Si(100), as was mentioned before. A similar gallium clumping together effect has been reported for the growth of GaAs on Si(100), and a lower binding-energy component was correspondingly observed.¹ The fact that the *S2* binding energy is fixed with respect to

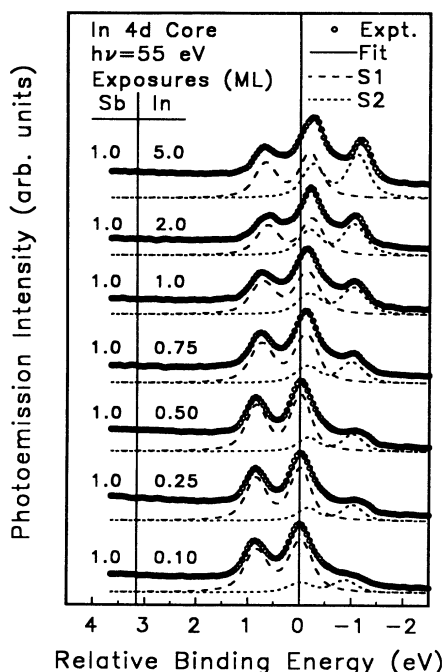


FIG. 5. In *4d* core-level spectra (open circles) taken with a photon energy of 55 eV. Successive In exposures deposited on a 1-ML-Sb-covered Si(100) surface are indicated for each spectrum. The solid curves are a result of a fit to the data. The decompositions of the spectra into the two surface contributions *S1* and *S2* are shown by the medium- and short-dashed curves, respectively.

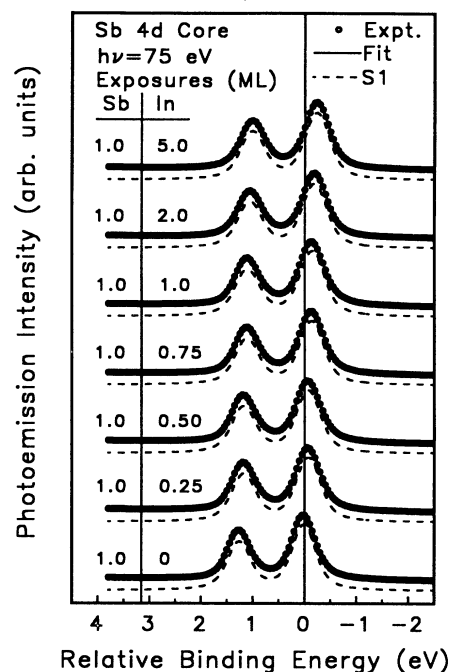


FIG. 6. Sb *4d* core-level spectra (open circles) taken with a photon energy of 75 eV. Successive In exposures deposited on a 1-ML-Sb-covered Si(100) surface are indicated for each spectrum. The solid curves are a result of a fit to the data. The decomposition of the spectra into the one surface contribution *S1* is shown by the medium-dashed curves. The relative binding energies are referenced to the Fermi level, which is located at -32.4 ± 0.1 eV.

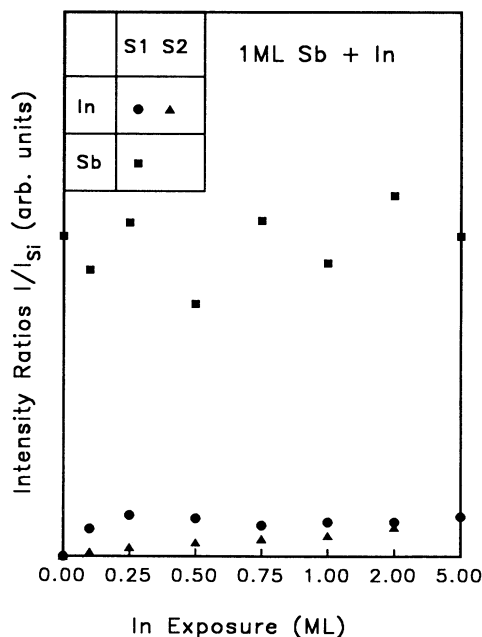


FIG. 7. In and Sb intensity ratios for each surface component, with respect to the Si bulk, are shown for various In exposures on a 1-ML-Sb-covered Si(100) surface. Circles and triangles indicate the results for the two In surface components. Squares show similar results for the Sb surface site.

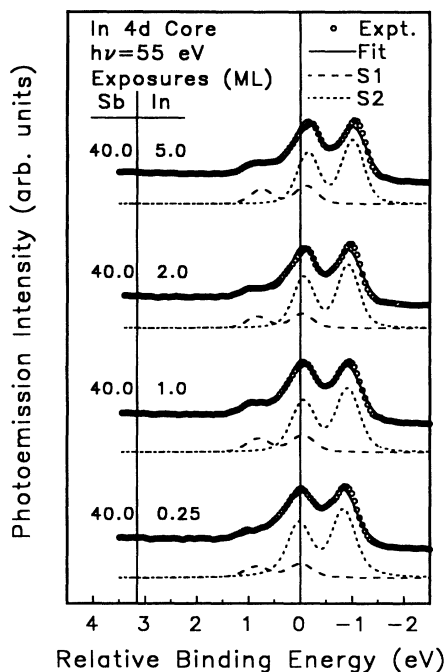


FIG. 8. In $4d$ core-level spectra (open circles) taken with a photon energy of 55 eV. Successive In exposures deposited on a 40-ML-Sb-covered Si(100) surface are indicated for each spectrum. The solid curves are a result of a fit to the data. The decompositions of the spectra into the two surface contributions S1 and S2 are shown by the medium- and short-dashed lines, respectively.

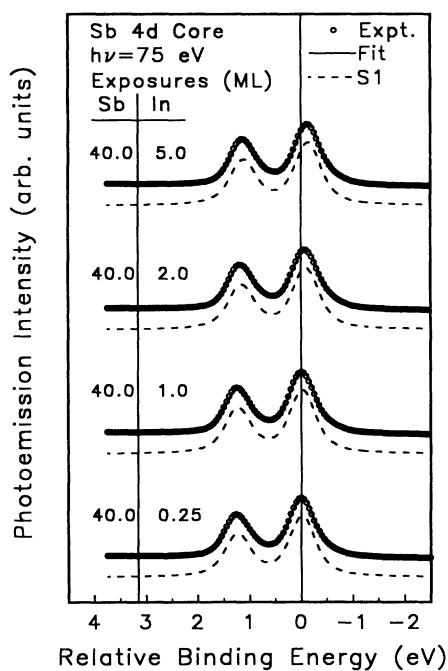


FIG. 9. Sb $4d$ core-level spectra (open circles) taken with a photon energy of 75 eV. Successive In exposures deposited on a 40-ML-Sb-covered Si(100) surface are indicated for each spectrum. The solid curves are a result of a fit to the data. The decomposition of the spectra into the one surface contribution S1 is shown by the medium-dashed lines.

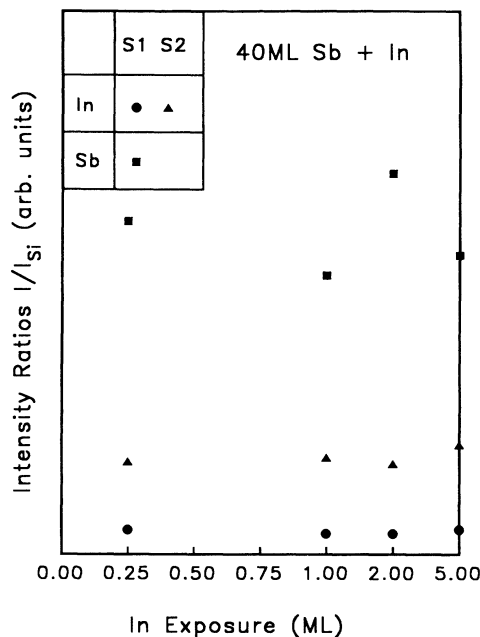


FIG. 10. In and Sb intensity ratios for each surface component, with respect to the Si bulk, are shown for various In exposures on a 40-ML-Sb covered Si(100) surface. Circles and triangles indicate the results for the two In surface components. Squares show similar results for the Sb surface site.

the Fermi level and equals that for bulk metallic In also indicates that this component is due to metallic islands and not another site bound to the Si, which would be tied to the valence band. Based on these results, we assign the S2 component in the In core-level spectra to be derived from metallic In islands on the surface. Figure 2 shows a similar core-level movement for the single chemical site of Sb due to Sb doping silicon n type.

The intensity ratios in Fig. 3 show that the S1 site for In diminishes for increasing Sb coverages, while the S2 component is slowly increasing. Therefore, the S2 site in Fig. 1 is seen to be increasing quite rapidly relative to the S1 site. Figure 4 presents the Si core for the clean and 1-ML coverage of In, Sb, and InSb. The surface component (S) for clean Si(100) is derived from atoms within the surface layer having a dangling bond. For the covered surfaces, the lack of a surface component indicates that all the Si dangling bonds have been saturated. Again, the movement of the core is due to p - or n -type doping of the surface with In or Sb, respectively.

Based on the results of HEED and the core-level deconvolution, we conclude that Sb-Si bonds are formed, breaking the initial In-Si bonds. Thus the HEED pattern changes from the In-terminated (3×4) to the Sb-terminated, disordered (1×1), and the In S1 site diminishes for increasing Sb exposures. The released In adatoms then migrate and stick to other In adatoms, causing an increase in the clumped together S2 site. Since the actual surface area covered by these three-dimensional In islands, on top of a mostly Sb-covered Si surface, is small, they would account for a small part of the photoemission spectra (see Fig. 3). Since the Sb core level only exhibits

one site $S1$, we conclude that Sb mostly bonds to Si with very little bonding to In.

To confirm that the first-layer bonding to Si is mostly Sb, we reversed the deposition order, putting 1 ML Sb down first and then exposing the surface to increasing amounts of In. Figures 5–7 show the photoemission results as described earlier. Figure 5 shows that In is again present in two sites $S1$ and $S2$. $S1$ moves relative to the Fermi level as a result of band bending, and $S2$ remains fixed with respect to the Fermi level. Figure 6 shows that Sb is again present in only one site. The intensity ratios in Fig. 7 are similar to Fig. 3 in that even after 1-ML In exposure the In $S1$ is still only about 0.1 ML. The tendency is for In to clump together, as seen by the increase in the $S2$ component. Even a direct comparison of the In core-level line shape between 1 ML In+1 ML Sb and 1 ML Sb+1 ML In shows them to be very similar. The only difference is in the magnitude of band bending. We find that the Fermi level moves, with respect to the clean surface, to 0.20 and 0.35 eV toward higher binding energy for 1 ML In+1 ML Sb and 1 ML Sb+1 ML In, respectively. Apart from this point, our conclusion from the first two sets of figures is simply that deposition order makes no difference on either on-axis Si(100) or vicinal Si(100); Sb preferentially bonds to Si, driving In to agglomerate with itself.

A further question is why does roughly 0.1 ML In still bond to the Si surface after more than one monolayer of Sb has been deposited on the 1-ML-In-deposited Si surface (see Fig. 3). We think two possible explanations exist: In is either bonding to defect sites or to step edges. If it bonds to step edges, then we should have seen a difference between vicinal and on-axis Si(100). Our 4° -off Si(100) sample increases the overall step area by at least a factor of 3, and this could easily be seen as an increase in the In $S1$ site. Since we did not this would imply that In is bonding to defect sites. A typical clean Si(100)-(2 \times 1) is covered with around 10% defect sites, and this fits nicely with the 0.1-ML In $S1$ sites left on the surface.²⁴ It is interesting to note that, in Fig. 5, In prefers to bond to these defects rather than agglomerating with other mobile In adatoms, as shown by the “filling in” of the $S1$ site before clumping together into the $S2$ site.

Another curious phenomenon in Fig. 3 seems to be the continual, slow decline of the In $S1$ site from its value at 1 ML Sb to 5 ML Sb. The results in Figs. 8–10 continue in the above-mentioned trend. After initially exposing the surface to 40 ML Sb, Fig. 8 shows that any In then deposited mostly clumps together; this should be compared with Fig. 5. The intensity ratio of the In $S1$ site, in Fig. 10, is now down to just a few percent of a monolayer. We know Sb saturates at 1 ML, and so how could the excess Sb affect those defect sites that could bond to In? One possible explanation is that the sticking probability, for the defect sites, is much lower for Sb than it is for In. However, with continual pounding of the surface with Sb, the defect sites are eventually saturated.

As a comparison to our results for InSb on Si(100), there are some similarities and differences to GaAs on Si(100). The deposition order, like GaAs, does not matter with As always diffusing to the surface and forming As-Si

bonds with probably 20% of the surface covered with Ga-Si bonds.^{1–3} One theoretical model predicts that the Si atoms at a double-layer step (DLS) are replaced by Ga atoms, creating pairs of fourfold-coordinated Ga and As atoms, which begin the nucleation of the GaAs islands.⁴ It could be that these 20% of Ga atoms bonded to Si are these very DLS Ga atoms. Anyway, for GaAs island growth most of the Ga, instead of clumping together like In, tends to bond to As. The energetics of these GaAs island formations are thought to be driven by this stability of the underlying As- or GaAs-terminating layer.⁵ Since As forms a stable (2 \times 1) reconstruction on Si and Sb does not (within our temperature range),^{18,25} the In atoms might tend to clump together rather than form covalent bonds with the underlying disordered Sb layer. This initial clumping together of In at the surface has consequences for the growth of InSb on Si(100), as we shall discuss in the next section.

B. Higher coverages

Our Si substrates were held at temperatures from 300°C to 520°C during growths between 50 and 600 ML of InSb. The Sb/In flux ratio was varied between 2 and 5. The final InSb coverage values quoted below refer to the amount of In evaporated. The deposition rate of Sb was held at around 0.5 Å/s. Both In and Sb prelayers of a few monolayers were used to initiate growth. HEED was used during deposition to monitor the long-range order of these thicker growths. After the Sb shutter was opened, HEED showed a pattern change to a (1 \times 1). Thereafter, the background slowly increased and the (1 \times 1) diffraction spots slowly decreased until only background was left. In all of our trials, no ordered InSb growth was ever observed with HEED, and in each case, except for the lowest-temperature growth where the film was shiny, a dull metallic film covered our Si substrate.

For the spectra in Figs 11–13, the relative Auger in-

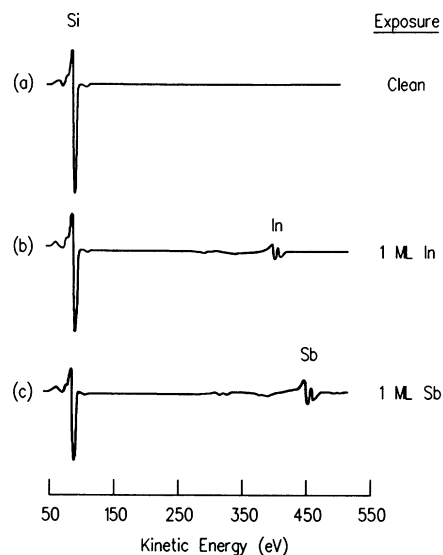


FIG. 11. Auger spectra showing (a) clean Si(100), (b) Si(100)+1 ML In deposited at 410°C, and (c) Si(100)+1 ML Sb deposited at 410°C.

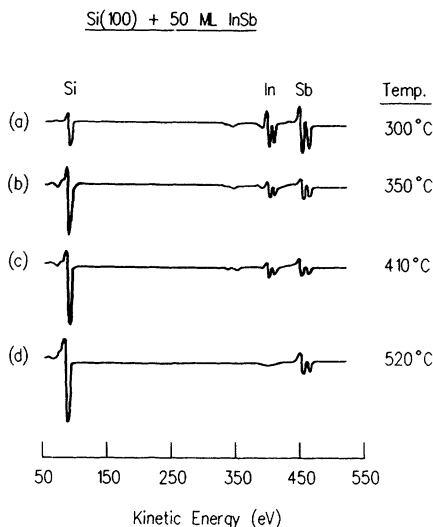


FIG. 12. Auger spectra of Si(100)+50 ML InSb for various deposition temperatures, as indicated.

tensities are plotted as a function of the Auger kinetic energies. The major Auger peak energy for the Si *LMM* transitions and the In and Sb *MNV* transitions are at 92, 404, and 454 eV, respectively. The intensities for different spectra can be directly compared. Figure 11 shows the spectra for clean Si and Si covered by one monolayer of In and Sb deposited at 410°C.

Figure 12 presents the Auger spectra for coverages of 50 ML InSb. The InSb was coevaporated onto substrates held at various temperatures between 300°C and 520°C, as indicated. The most striking feature of all the spectra is the continued appearance of the Si Auger signal, which shows that the growth is certainly not ideal. Spectra (b) and (c) of Fig. 12 tell us that the Auger signal corre-

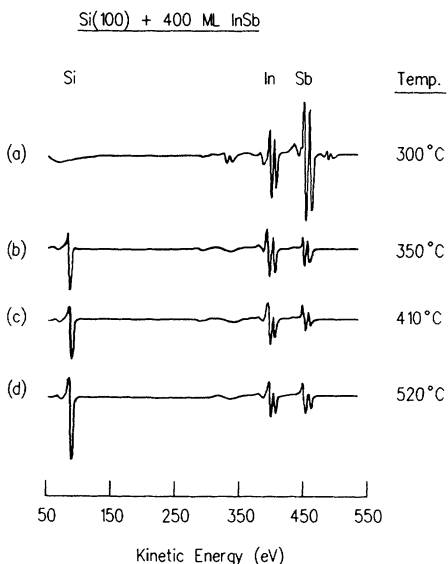


FIG. 13. Auger spectra of Si(100)+400 ML InSb for various deposition temperatures, as indicated.

sponds to only about a monolayer of Sb. From our low-coverage results presented above, we know that Sb bonds to the Si surface, causing the In to clump together. The In Auger signal is therefore due to these metallic islands. For a uniform 50-ML In film, the In Auger signal should be ~5–10 times as intense as a uniform 1-ML film based on an escape-depth consideration. Since the In signal strength is only about the same as that for a 1-ML film, we conclude that the In islands cover only ~10–20% of the surface area. In spectrum (d) of Fig. 12, only the Sb signal is seen and is due to the reduced sticking probability of In in this temperature range.¹⁶ For spectrum (a) of Fig. 12, the In and Sb signals are stronger, with a diminished Si peak. We will have more to say about this low-temperature growth phase.

Figure 13 shows similar results, except that we deposited 400 ML of InSb. Spectra (b)–(d) of Fig. 13 are very similar and show the continued three-dimensional growth of In on top of a monolayer of Sb. If these islands were due to InSb and not just In, then we would expect both the In and Sb signal to increase in a similar way from the 50–400-ML exposures. Since only the In signal increases, we conclude that these islands are just due to In. Spectrum (a) of Fig. 13 shows a much thicker “InSb” layer. The escape depth for the Auger electrons is around 10–30 Å, and so the film is at least several times that thick since no Si signal is observed. X-ray diffraction was performed on this film, and the results are shown in Fig. 14. The *d* values, and the corresponding element or compound for these peaks, are presented in Table I. We find that the sample has some polycrystalline InSb, but is overwhelmingly made up of Sb polycrystals. This explains why the Sb signal was large in the Auger spectrum (a) in Fig. 13. Also, since some InSb was

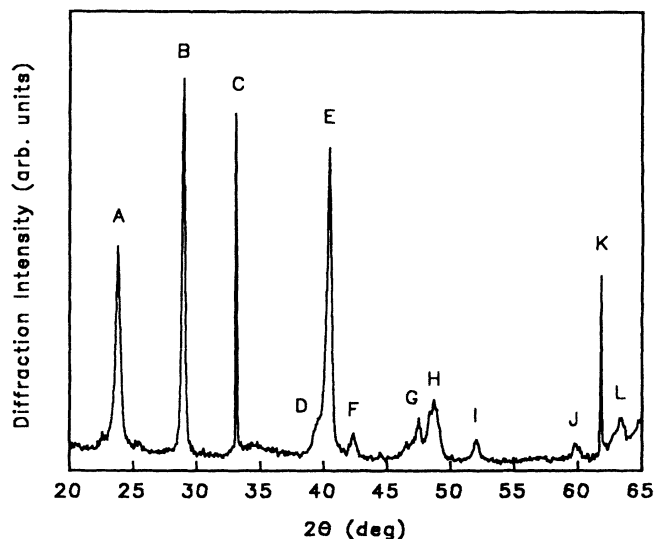


FIG. 14. X-ray-diffraction data of Si(100)+400 ML InSb grown at 300°C. The diffraction intensity is shown as a function of 2θ . No peaks were found below 20°, while from 65° to 75° the Si(400) peak obscures any other useful data. Peaks are labeled with letters from A–L.

TABLE I. From Fig. 14, the d values for each peak were determined from the 2θ values and Bragg's law. The uncertainty in the d value, due to the uncertainty in the peak position, is ± 0.015 Å. The material was determined from a comparison of the d values with InSb and Sb powder diffraction data.

Peak	2θ (deg)	d (Å)	Material	hkl
A	23.87	3.73	InSb	111
B	28.85	3.10	Sb	012
C	33.08	2.71	Si	400 ^a
D	39.50	2.28	InSb	110
E	40.24	2.24	Sb	104
F	42.30	2.14	Sb	110
G	47.41	1.92	Sb	015
H	48.68	1.87	Sb	006
I	52.04	1.77	Sb	202
J	59.91	1.55	Sb	024
K	61.78	1.50	Si	400 ^b
L	63.36	1.47	Sb	107

^aAt $\frac{1}{2}K\alpha$.

^bDue to $K\beta$.

formed, the increase in the In signal is explained. We also tried growing more InSb at 410°C on top of this film—however, HEED did not show any ordered InSb growth.

As we mentioned previously, high-quality InSb films can be grown on InSb(100), CdTe(100), etc., in the temperature range we investigated. In addition to the above-mentioned experiments, we also tried growing InSb on disordered and oxygenated Si(100) surfaces as well as growing InSb prelayers at room temperature before higher-temperature growths. Needless to say, we were not able to grow ordered InSb films on Si(100) for any exposures up to 600 ML of coevaporated InSb. This is not to say that, by depositing much larger quantities of InSb on Si(100), ordered films would not eventually grow. Other workers have indeed grown InSb on Si(100) for coverages of 3.2 μm at 410°C.²⁶

IV. CONCLUSION

We analyzed the initial interface formation between InSb and Si(100). It was found that Sb preferentially bonds to Si, displacing the chemisorbed In atoms and causing it to agglomerate with itself. The remaining In on the Sb-terminated surface, which did not form metallic islands, were thought to be bound to defect sites on the Si surface. Ordered InSb films up to 600 ML thick, in the temperature range between 350°C and 520°C, could not be grown on the Si(100) surface because of the interfacial interactions, which induce In to form metallic islands on a Sb-terminated, disordered (1×1) surface. Below 350°C, a slight amount of InSb is present, but mostly bulk Sb polycrystals are formed. It might be that with a judicious choice of temperature and a Sb/In flux ratio, quality InSb films could be grown, but the growth is certainly much more difficult than for the GaAs-on-Si system.

ACKNOWLEDGMENTS

This material is based upon work supported by the U.S. Department of Energy (Division of Materials Sciences, Office of Basic Energy Sciences), under Grant No. DEFG02-91ER45439. Acknowledgement is also made to the donors of the Petroleum Research Fund, administered by the American Chemical Society, and to the U.S. National Science Foundation (Grant No. DMR-89-19056) for partial personnel and equipment support. We acknowledge the use of central facilities of the Materials Research Laboratory of the University of Illinois, which is supported by the U.S. Department of Energy (Division of Material Sciences, Office of Basic Energy Sciences), under Grant No. DEFG02-91ER45439, and the U.S. National Science Foundation under Grant No. DMR-89-20538. The Synchrotron Radiation Center is supported by the U.S. National Science Foundation.

*Permanent address: Department of Materials Science, University of Southern California, Los Angeles, CA 90089.

¹R. D. Bringans, M. A. Olmstead, R. I. G. Uhrberg, and R. Z. Bachrach, Phys. Rev. B **36**, 9569 (1987).

²R. D. Bringans, M. A. Olmstead, R. I. G. Uhrberg, and R. Z. Bachrach, Appl. Phys. Lett. **51**, 523 (1987).

³H. Okumura, Y. Suzuki, K. Miki, K. Sakamoto, T. Sakamoto, S. Misawa, and S. Yoshida, J. Vac. Sci. Technol. B **7**, 481 (1989).

⁴Efthimios Kaxiras, O. L. Alerhand, J. D. Joannopoulos, and G. W. Turner, Phys. Rev. Lett. **62**, 2484 (1989).

⁵John E. Northrup, Phys. Rev. Lett. **62**, 2487 (1989).

⁶R. Fischer, W. T. Masselink, J. Klem, T. Henderson, T. C. McGlenn, M. V. Klein, H. Morkoç, and J. Washburn, J. Appl. Phys. **58**, 374 (1985).

⁷R. Fischer, H. Morkoç, D. A. Neumann, H. Zabel, C. Choi, N. Otsuka, M. Longerbone, and L. P. Erickson, J. Appl. Phys. **60**, 1640 (1986).

⁸D. K. Biegelsen, F. A. Ponce, A. J. Smith, and J. C. Tramonta-

na, J. Appl. Phys. **61**, 1856 (1987).

⁹M. Kawabe, T. Ueda, and H. Takasugi, Jpn. J. Appl. Phys. **26**, L114 (1987).

¹⁰M. Yata, Thin Solid Films **137**, 79 (1986).

¹¹R. Hull and A. Fischer-Colbrie, Appl. Phys. Lett. **50**, 851 (1987).

¹²P. John, T. Miller, and T.-C. Chiang, Phys. Rev. B **39**, 1730 (1989); P. John, Ph.D. thesis, University of Illinois at Urbana-Champaign, 1988.

¹³K. Oe, S. Ando, and K. Sugiyama, Jpn. J. Appl. Phys. **19**, L417 (1980).

¹⁴J. L. Glenn, Jr., Sungki O, L. A. Kolodziejki, R. L. Gunshor, M. Kobayashi, D. Li, N. Otsuka, M. Haggerott, N. Pelekanos, and A. V. Nurmikko, J. Vac. Sci. Technol. B **7**, 249 (1989).

¹⁵A. J. Noreika, M. H. Francombe, and C. E. C. Wood, J. Appl. Phys. **52**, 7416 (1981).

¹⁶J. Knall, J.-E. Sundgren, G. V. Hansson, and J. E. Greene, Surf. Sci. **166**, 512 (1986).

- ¹⁷A. A. Baski, J. Nogami, and C. F. Quate, *Phys. Rev. B* **43**, 9316 (1991).
- ¹⁸D. H. Rich, F. M. Leibsle, A. Samsavar, E. S. Hirschorn, T. Miller, and T.-C. Chiang, *Phys. Rev. B* **39**, 12 758 (1989).
- ¹⁹S. A. Barnett, H. F. Winters, and J. E. Greene, *Surf. Sci.* **165**, 303 (1986).
- ²⁰T.-C. Chiang, *CRC Crit. Rev. Solid State Mater. Sci.* **14**, 269 (1988).
- ²¹G. E. Franklin, D. H. Rich, A. Samsavar, E. S. Hirschorn, F. M. Leibsle, T. Miller, and T.-C. Chiang, *Phys. Rev. B* **41**, 12 619 (1990).
- ²²D. H. Rich, A. Samsavar, T. Miller, H. F. Lin, T.-C. Chiang, J.-E. Sundgren, and J. E. Greene, *Phys. Rev. Lett.* **58**, 579 (1987).
- ²³D. H. Rich, G. E. Franklin, F. M. Leibsle, T. Miller, and T.-C. Chiang, *Phys. Rev. B* **40**, 11 804 (1989).
- ²⁴R. J. Hamers, R. M. Tromp, and J. E. Demuth, *Phys. Rev. B* **34**, 5343 (1986).
- ²⁵J. Nogami, A. A. Baski, and C. F. Quate, *Appl. Phys. Lett.* **58**, 475 (1991). By depositing Sb on Si(100) at about 550 °C a (2×1) reconstruction is formed. If the deposition is done at lower temperatures (such as the temperatures used in our study), the surface becomes disordered.
- ²⁶J.-I. Chyi, D. Biswas, S. V. Iyer, N. S. Kumar, H. Morkoç, R. Bean, K. Zanio, H.-Y. Lee, and Haydn Chen, *Appl. Phys. Lett.* **54**, 1016 (1989).